Dynamic scaling in phase separation kinetics for quasi-two-dimensional membranes

Brian A. Camley and Frank L. H. Brown

Citation: The Journal of Chemical Physics **135**, 225106 (2011); doi: 10.1063/1.3662131
View online: http://dx.doi.org/10.1063/1.3662131
View Table of Contents: http://scitation.aip.org/content/aip/journal/jcp/135/22?ver=pdfcov
Published by the AIP Publishing

Dynamic scaling in phase separation kinetics for quasi-two-dimensional membranes

Brian A. Camley[1,a)] and Frank L. H. Brown[1,2,a)]
[1]*Department of Physics, University of California, Santa Barbara, California 93106, USA*
[2]*Department of Chemistry and Biochemistry, University of California, Santa Barbara, California 93106, USA*

(Received 1 August 2011; accepted 27 October 2011; published online 14 December 2011)

We consider the dynamics of phase separation in lipid bilayer membranes, modeled as flat two-dimensional liquid sheets within a bulk fluid, both in the creeping flow approximation. We present scaling arguments that suggest asymptotic coarsening in these systems is characterized by a length scale $R(t) \sim t^{1/2}$ for critical (bicontinuous) phase separation and $R(t) \sim t^{1/3}$ for off-critical concentrations (droplet morphology). In this limit, the bulk fluid is the primary source of dissipation. We also address these questions with continuum stochastic hydrodynamic simulations. We see evidence of scaling violation in critical phase separation, where isolated circular domains coarsen slower than elongated ones. However, we also find a region of apparent scaling where $R(t) \sim t^{1/2}$ is observed. This appears to be due to the competition of thermal and hydrodynamic effects. We argue that the diversity of scaling exponents measured in experiment and prior simulations can in part be attributed to certain measurements lying outside the asymptotic long-length-scale regime, and provide a framework to help understand these results. We also discuss a few simple generalizations to confined membranes and membranes in which inertia is relevant. © *2011 American Institute of Physics*. [doi:10.1063/1.3662131]

I. INTRODUCTION

The dynamics of phase separation in binary (and effectively binary) systems is a rich field of study.[1–3] Coarsening is often characterized by dynamical scaling laws,[1,4–6] which predict physical properties that depend on time only through a single emergent length scale, $R(t)$. Systems obeying dynamical scaling show self-similarity, in the sense that evolution in time is statistically equivalent to a rescaling in space. Such behavior has been well established in certain cases such as alloys and the "diffusive growth" regime in binary fluids.[1] In other systems, dynamical scaling is violated. For example, two-dimensional (2D) binary fluids in the "viscous hydrodynamic regime" (characterized by low Reynolds number "creeping" flow) violate the scaling hypothesis.[7–9]

We study phase separation in a multicomponent lipid bilayer membrane. A membrane is often described as a "quasi-two-dimensional fluid",[10,11] in which the fluid flow within the two-dimensional membrane is coupled to the flow of a less viscous three-dimensional (3D) fluid surrounding the membrane. Many of the anomalies of two-dimensional fluid flow at low Reynolds numbers are altered by the presence of the bulk fluid. For instance, the diverging mobility of a particle in a 2D fluid at zero Reynolds number (Stokes paradox) (Ref. 12) is regulated by the outside fluid viscosity,[10] and the slow ($\sim t^{-1}$) decay of velocity autocorrelations in 2D fluids[13,14] crosses over to a $t^{-3/2}$ behavior in membranes.[15]

Phase separation within membranes is of theoretical interest because the quasi-2D geometry incorporates both 2D and 3D fluid flow; the dynamics of interest are confined to a plane, while the viscous dissipation extends to 3D space. Quasi-2D hydrodynamics is known to be relevant for the diffusion of membrane-embedded objects, as proteins[16] as well as larger bodies within membranes[17] have diffusion coefficients in agreement with quasi-2D hydrodynamic theory.[10,18] Beyond simple diffusion, the quasi-2D hydrodynamics also affects the dynamics of hydrodynamic correlations of particles in a membrane,[11] membrane domain fluctuations,[19,20] and the dynamics of critical fluctuations in membranes.[21–23] This fluid geometry also has broader importance in the context of lipid monolayers,[24] colloidal particles at interfaces,[25] and thin liquid crystal films.[26]

Equally strong motivation for the study of dynamics in multicomponent lipid bilayers is biological/biophysical. An interest in the biological activity of lipid rafts[27,28] has motivated the experimental study of phase separation in multicomponent "model membrane" systems,[29,30] including the measurement of scaling exponents.[31–33] Recent simulations have also addressed these questions,[34–37] demonstrating the importance of hydrodynamics in the coarsening process. However, reported scaling exponents and even the presence of scaling vary from paper to paper, and no framework exists for interpreting these results. Comparison between these different simulations is in part confounded by the limitations of each approach. Dissipative particle dynamics simulations[34,35] may have unphysically low membrane viscosities; in particular, Ramachandran *et al.*[35] note that their membrane viscosity is of the order of their water viscosity. Binary fluid models allow both membrane and outer fluid viscosity to be changed, but lack molecular details; the simulations of Fan *et al.*,[37] which display scaling violation, do not include thermal fluctuations. Though thermal fluctuations are believed to be asymptotically

a)Authors to whom correspondence should be addressed. Electronic mail: camley@physics.ucsb.edu and flbrown@chem.ucsb.edu.

irrelevant in the coarsening of many systems, they play a role in the coarsening of binary fluids by driving coalescence,[1] which is the primary observed mechanism of phase separation in off-critical lipid membranes.[29] To understand coalescence dynamics and address the inconsistencies between earlier simulations, it is important to simulate systems including thermal fluctuations.

Our simulation technique, first introduced in Ref. 36, uses hydrodynamic equations with Langevin forces that obey a fluctuation-dissipation theorem, reproducing known equilibrium and dynamic behavior for membranes. This allows us to explicitly look at coarsening dynamics for both critical and off-critical systems, including the diffusion and coalescence mechanism. We also present simple scaling laws that are consistent with observed scaling exponents where dynamical scaling is present, and use these scaling laws to clarify regimes where different coarsening mechanisms should dominate. We also identify where scaling laws appear to be violated.

As is customary,[1] we describe phase separation via a composition phase field $\phi(\mathbf{r})$ (e.g., $\phi = \chi_A - \chi_B$ for a mixture of A and B, where χ_i are mole fractions) and a standard Landau-Ginsburg free energy for binary mixtures $H = \int d^2r[-\frac{\epsilon}{2}\phi^2 + \frac{u}{4}\phi^4 + \frac{\gamma}{2}|\nabla\phi|^2]$.[1,5] The field is confined to a flat geometry, $\mathbf{r} = (x, y)$, and the parameters ϵ, u, and γ are determined by the physical observables σ, the line tension between coexisting phases, ξ, the interface width, and ϕ_0, the equilibrium composition of one phase. The field evolves via overdamped model H (Refs. 1 and 5) dynamics,

$$(\partial_t + \mathbf{v}\cdot\nabla)\phi(\mathbf{r},t) = M\nabla^2\frac{\delta H}{\delta\phi(\mathbf{r},t)} + \theta(\mathbf{r},t)$$
$$v_i(\mathbf{r},t) = \int d^2r'\, T^m_{ij}(\mathbf{r}-\mathbf{r}') \times\left[\frac{\delta H}{\delta\phi}\nabla'_j\phi(\mathbf{r}',t) + \zeta_j(\mathbf{r}',t)\right]. \quad (1)$$

The transport coefficient M is related to the bulk concentration diffusion coefficient $D_\phi = 2M\epsilon$ and the tensor $T^m_{ij}(r)$ is the Green's function for velocity response to an applied point force in the membrane plane (see Eq. (2)). $\theta(\mathbf{r}, t)$ and $\zeta_j(\mathbf{r}, t)$ are Gaussian white random forces with variances chosen to satisfy the fluctuation-dissipation theorem; the multiplicative noise inherent to Eq. (1) must be interpreted within the Stratonovich convention (see Appendix). We will evolve Eq. (1) numerically on an $N \times N$ lattice; $N = 1024$ for all simulations presented in this paper. The theoretical framework is identical to that described in Ref. 36 and readers are referred there for further details, especially concerning numerical solution of the equations.

We adopt the Saffman-Delbrück hydrodynamic model,[10] treating the membrane as a thin 2D fluid, immersed within a lower viscosity bulk fluid. This leads to a crossover in $T^m_{ij}(\mathbf{r})$ whereby forces are transmitted via the membrane over short distances and by the outside fluid at longer distances.[24] This behavior is most clearly apparent in the Fourier transform of $T^m_{ij}(\mathbf{r})$, $T^m_{ij}(\mathbf{q}) \equiv \int d^2r\, T^m_{ij}(\mathbf{r})e^{-i\mathbf{q}\cdot\mathbf{r}}$,

$$T^m_{ij}(\mathbf{q}) = \frac{1}{\eta_m(q^2 + q/L_{sd})}\left(\delta_{ij} - \frac{q_iq_j}{q^2}\right), \quad (2)$$

where the Saffmann-Delbrück length scale $L_{sd} = \eta_m/2\eta_f$ is set by the ratio of the membrane surface viscosity η_m and the outside fluid viscosity η_f. Equation (2) reduces to the purely 2D response $T^m(r) \sim \ln(r)$ for $r \ll L_{sd}$, but behaves as $T^m(r) \sim 1/r$, characteristic of 3D fluid response, when $r \gg L_{sd}$. Although the dynamics contained within Eqs. (1) and (2) are confined to a 2D plane, they are governed by implicit hydrodynamic flows in 3D and will be referred to as "quasi-2D" henceforth. For convenience, we will refer to the two limiting hydrodynamic regimes mentioned above as the "2D" and "3D" limits of the quasi-2D model. Other parameters, such as the transport coefficient M and the temperature will also affect scaling behavior; we present the various regimes of the model described by Eq. (1) in Table I.

II. SCALING THEORIES OF COARSENING IN A QUASI-2D MEMBRANE

A. Dynamical scaling

The dynamical scaling hypothesis implies that the structure function $S(\mathbf{q}, t) = \langle\phi_{\mathbf{q}}(t)\phi_{-\mathbf{q}}(t)\rangle$ only depends on time through a single, emergent length scale $R(t)$,[1,4]

$$S(\mathbf{q},t) = R^d(t)\, g\,(q\,R(t))\,, \quad (3)$$

where $g(x)$ is a scaling function dependent only on x, and d is the dimensionality of the space where $\phi(\mathbf{r}, t)$ is specified ($d = 2$ in our case). The dependence of $R(t)$ on t is often taken to be a simple power law, $R(t) \sim t^\alpha$. Dynamical scaling is well-established for binary alloys, and several regimes of binary fluids, and in many cases the dynamical exponents α can be extracted by simple scaling analysis.[1] We extend these classical results to phase separation in a simple model membrane.

Assuming dynamical scaling holds, the only relevant length scale is $R(t)$ and it becomes possible to estimate the various contributions to Eq. (1) in a scaling sense, e.g., $\nabla \sim 1/R(t)$, $d^2r \sim R^2(t)$. The term $\delta H/\delta\phi$ has units of energy per area; if the line tension σ is driving the coarsening, then $\delta H/\delta\phi \sim \sigma/R(t)$. The Oseen tensor has two characteristic regimes, $T^m \sim \eta_m^{-1}\ln R(t)$ for $R \ll L_{sd}$ and $T^m \sim 1/\eta_f R(t)$ for $R \gg L_{sd}$.

If we apply these scaling rules to the velocity part of Eq. (1), we find $R(t) \sim t$ up to logarithmic corrections for $R \ll L_{sd}$, the 2D viscous (2DV) regime, and $R(t) \sim t^{1/2}$ for $R \gg L_{sd}$, the 3D viscous (3DV) regime. We see that the dynamics of systems below and above the Saffman-Delbrück length are expected to be quantitatively and qualitatively different. Our scaling theory predicts $\alpha = 1$ for $R \ll L_{sd}$ (2DV). This is also the scaling theory result for ordinary binary fluids in the viscous limit, independent of dimension.[1] However, numerical simulations are consistent with $\alpha = 1$ in three-dimensional simple binary fluids,[38] but scaling is violated in two-dimensional binary fluids in the viscous limit,[7,9]

TABLE I. Summary of dynamical scaling properties. Theoretical predictions from scaling laws are presented as simple fractions. Simulated exponents are extracted from fitting $R_1(t)$ as extracted from Eq. (5). In the viscous critical mixtures, (†), scaling violation is observed for some parameters. Uncertainties given are a combination of systematic uncertainty from varying n in Eq. (5) and the fitting range, and the statistical variation in α. Large systematic errors are observed for coalescence regimes, but it is unclear if this is due to violation of scaling or limited simulation length. $\langle\phi\rangle = -0.2$ in all off-critical simulations.

Regime	α (scaling theory)	α (simulation)
Critical mixture ($\langle\phi\rangle = 0$)		
$R \ll L_{sd}$ (2D regime)		
$R(t) \ll \sqrt{M\eta_m}$	2D Cahn-Hilliard (2DCH)	1/3	0.34 ± 0.02
$R(t) \gtrsim \sqrt{M\eta_m}$	2D viscous (2DV)	1	†
$R(t) \gg L_{sd}$ (3D regime)		
$R(t) \ll M\eta_f$	3D Cahn-Hilliard (3DCH)	1/3	0.35 ± 0.02
$R(t) \gg M\eta_f$	3D viscous (3DV)	1/2	†
Off-critical mixture ($\langle\phi\rangle \neq 0$)		
$R \ll L_{sd}$ (2D regime)		
$R(t) \ll \eta_m M\sigma/k_BT$	2D Ostwald ripening (2DO)	1/3	0.32 ± 0.02
$R(t) \gtrsim \eta_m M\sigma/k_BT$	2D coalescence (2DC)	1/2	0.47 ± 0.08
$R(t) \gg L_{sd}$ (3D regime)		
$\sigma M\eta_f \gg k_BT$	3D Ostwald ripening (3DO)	1/3	0.32 ± 0.04
$\sigma M\eta_f \ll k_BT$	3D coalescence (3DC)	1/3	0.30 ± 0.09

suggesting that our scaling analysis may be insufficient in the limit $R \ll L_{sd}$.

There are several well-known complications to this basic picture: these scaling laws are only expected to be relevant for critical concentrations ($\langle\phi\rangle = 0$),[1] and temperature may play a role.[1,39] We can address the relevance of these issues by applying the renormalization group technique of Bray.[1] We coarse-grain the field ϕ by eliminating modes $\phi_{\mathbf{k}}(t)$ with $\Lambda/b < k < \Lambda$, where $\Lambda \sim 1/\xi$ is an ultraviolet cutoff. We rescale the equations of motion (Eq. (1)) and look for fixed points, which determine the asymptotic scaling of $R(t)$. Bray notes that though this elimination step of renormalization cannot be carried out, the $k \to 0$ singularity (due to the local conservation of material) cannot be changed by removing "hard" large-k Fourier components $\phi_{\mathbf{k}}(t)$, which allows the recursion relations for a scaling fixed point to be written down. This does assume the existence of a scaling fixed point, and so may produce incorrect results in limits where the scaling hypothesis breaks down.

We apply this procedure in the 3D regime ($T^m(r) \sim 1/\eta_f r$), which gives renormalization equations,

$$M' = b^{\frac{1}{\alpha}-3}M,$$
$$\left(\frac{1}{\eta_f}\right)' = b^{\frac{1}{\alpha}-2}\left(\frac{1}{\eta_f}\right),$$
$$T' = b^{-1}T. \tag{4}$$

These recursion relations show that in the 3D limit, the Cahn-Hilliard (3DCH) fixed point, $\alpha = 1/3$, is unstable to the introduction of hydrodynamic interactions. Instead, asymptotic scaling dynamics are controlled by the $\alpha = 1/2$ viscous fixed point (3DV), where bulk diffusion (as described by M) is irrelevant. This is consistent with our scaling estimates. These results apply only to mixtures with $\langle\phi\rangle = 0$. For off-critical concentrations, the bicontinuous morphology is replaced by droplets and hydrodynamic effects are suppressed;[1] the $\alpha = 1/3$ fixed point is expected to be restored asymptotically.

Thermal fluctuations complicate this analysis for off-critical coarsening. The mechanism of the "diffusive" regime is Ostwald ripening / Lifshitz-Slyozov-Wagner (LSW) evaporation-condensation.[1] Finite temperature causes domain coalescence to compete with ripening. If there is only one length scale $R(t)$ in the problem, then $R(t)^2 \sim Dt$, where D is the diffusion coefficient of a domain of size R. In a quasi-2D fluid, $D \sim \ln(L_{sd}/R)$ for $R \ll L_{sd}$ and $D \sim 1/R$ for $R \gg L_{sd}$.[40,41] This would suggest $R(t) \sim (k_BTt/\eta_m)^{1/2}$ ($\alpha = 1/2$) in the 2D coalescence (2DC) regime, up to logarithmic corrections, but $R(t) \sim (k_BTt/\eta_f)^{1/3}$ ($\alpha = 1/3$) in the 3D coalescence (3DC) regime. These scaling results have also been noted by earlier papers.[37,42] For the 3D limit, the scaling exponents for diffusive growth and coalescence are identical, as in pure 3D fluids. This results from T/η_f being a *marginal* variable at the diffusive ($\alpha = 1/3$) fixed point in the renormalization treatment above.

To determine which regime a phase-separating system is in, we apply our earlier scaling estimates to Eq. (1), and determine the relative magnitude of the advective and diffusive terms. The magnitude of the advective term is $\sigma T^m(R)/R$, and the diffusive term is $M\sigma/R^3$, where $T^m(R)$ is the order of magnitude of the Oseen tensor: $T^m(R) \sim 1/(\eta_f R)$ for $R \gg L_{sd}$ (3D regime), and $T^m(R) \sim \ln(R/L_{sd})/\eta_m$ for $R \ll L_{sd}$ (2D regime). Therefore, we expect advection to be negligible when $R \ll M\eta_f$ in the 3D regime, and when $R \ll \sqrt{M\eta_m}$ in the 2D regime. We can calculate the relative importance of coalescence and the LSW evaporation-condensation mechanism similarly, by comparing the length scales for coalescence with the evaporation-condensation length scale $R(t) \sim (M\sigma t)^{1/3}$. These results are summarized in Table I.

B. Caveats of scaling

The scaling approach begins with the assumption of the dynamical scaling form, Eq. (3). We note that this scaling form is only a hypothesis, primarily supported by numerical simulation, and only established exactly for a few one-dimensional systems.[1] When would we expect the scaling hypothesis to be true? We have assumed that the only relevant length scale is the emergent length scale $R(t)$, which obviously requires that $R(t) \gg \xi$ (ξ is the thermal correlation length), as well as $R(t) \ll L_{\rm sys}$. In addition, we would not expect scaling if $R(t)$ is close to the Saffman-Delbrück length L_{sd}, i.e., scaling is only likely if $R(t) \ll L_{sd}$ or $R(t) \gg L_{sd}$.

Less obviously, other emergent length scales can appear if bulk diffusion is slow relative to hydrodynamic flows, leading to systems where there are deviations from the equilibrium concentrations $\pm\phi_0$ over large regions of space.[43,44] We see this in our simulations in certain limits, in which the interfaces become "smeared" over a large region, and as they are not in local equilibrium, secondary phase separations[44] can occur (see Fig. 2 at $k_BT = 0$). Scaling will only be seen if diffusion is fast enough to preserve the concentration profile near the interface in local equilibrium;[38] this is effectively the "sharp interface" limit for phase-field simulations used to simulate multiphase flow.[45] Of course, if local diffusion is too fast (large M), we will be close to the diffusion-dominated (Cahn-Hilliard) regime, which may lead to inaccuracies; this is the "residual diffusion" problem, which is well addressed in Kendon *et al.*[38] These issues are also important to the coalescence limit, but with an additional feature; even if we set the viscosities η_m and η_f to be infinite, if $M \neq 0$, the domain will still diffuse due to the stochastic term in Eq. (1).

III. SIMULATION RESULTS

A. Importance of thermal fluctuations

Thermal fluctuations, though generally believed to be irrelevant at long times in coarsening, can drive coalescence in binary fluids. At the first, qualitative level, we compare phase separation in membranes with and without thermal fluctuations, using realistic parameters. We simulate phase separation from an initially homogeneous state with $\langle\phi\rangle = 0$ by application of Eq. (1). We select parameters to model experiments on ternary giant unilamellar vesicles; these parameters are known to reproduce the experimental time scale and morphology, and are consistent with measured viscosities and line tensions.[36] We also perform an analogous simulation, but with thermal fluctuations turned off (Fig. 1). For this simulation, we choose an initial state with $\langle\phi\rangle = 0$ with small Gaussian fluctuations, with a standard deviation of 0.01; a perfectly homogeneous state has no gradients, and is thus a steady state of Eq. (1) if $k_BT = 0$.

Two features of phase separation at $k_BT = 0$ are obvious from Fig. 1: the coarsening process is slower than the finite-temperature result (note the different time scales), and there are more small domains at long times. The altered time for coarsening is largely due to the initial time required to form the bicontinuous structure, which is long due to the small influence of bulk diffusion in this system (i.e.. the Peclet number $\mathrm{Pe} = Lv/D_\phi$ is large, where L and v are characteristic length and velocity scales, and D_ϕ the diffusion coefficient). The relatively large population of small domains is unsurprising, as in two-dimensional binary fluids in the viscous limit, isolated domains coarsen at a slower rate than the bicontinuous structure.[7] The absence of thermal fluctuations removes a coalescence mechanism for the coarsening of these isolated domains. We also note that the excess small domains are not merely an artifact of the different time scales; there are no additional domain mergers in the $k_BT = 0$ simulation up to at least 100 s (data not shown).

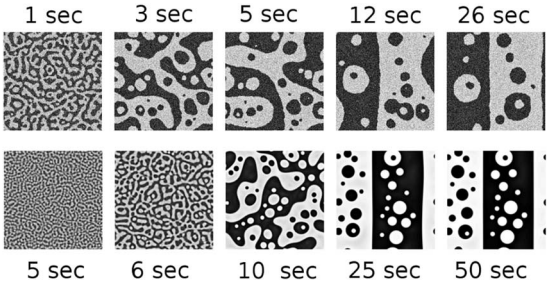

FIG. 1. Thermal fluctuations are important to the dynamics of systems parameterized to model real experimental conditions. Both top and bottom images are snapshots of the coarsening process in the model system described in Ref. 36, based on DOPC/DPPC/cholesterol vesicles. The top images are from a simulation that includes the effect of thermal fluctuations with $T = 21\,^\circ$C ($k_BT = 4.061$ pN nm), while the bottom images are from a simulation with no fluctuations, $k_BT = 0$. Including thermal fluctuations speeds up coarsening and provides an alternative route for isolated domains to coarsen, leading to fewer domains at long times. For this simulation, $\eta_m = 5 \times 10^{-6}$ surface Poise (s.P. or Poise cm) $\eta_f = 0$, line tension $\sigma = 0.1$ pN, interface width $\xi = 40$ nm, and system size of 30 μm $\times$ 30 μm. The concentration diffusion coefficient $D_\phi = 2M\epsilon = 6.5 \times 10^{-10}$ cm^2/s. Top: $k_BT = 4.061$ pN nm, $\Delta t = 20$ μs. This simulation is an extended run of the one presented in Ref. 36. Bottom: $k_BT = 0$, $\Delta t = 50$ μs.

We also note that in the limit of $k_BT = 0$, the order parameter does not take on its equilibrium values $\pm\phi_0$, even far away from the interface, until roughly $\sim$25 s, and there are gradients in ϕ over length scales much larger than the interface length. As noted in earlier sections, we would not necessarily expect to see scaling if diffusion is much slower than the hydrodynamics (large Peclet number), and this is one case of this effect. If we reduce the membrane viscosity or decrease the diffusion coefficient, we can exaggerate this violation of scaling (Fig. 2). This limit has been well-explored by Vladimirova *et al.*[43] for a two-dimensional binary fluid. However, this regime may not be physical; to obtain the extreme behavior of Fig. 2, we have chosen a membrane viscosity two orders of magnitude below those measured in Ref. 20, while keeping the concentration diffusion coefficient far below the expected order of magnitude of $k_BT/4\pi\eta_m$. This behavior is also completely destroyed by including thermal fluctuations (Fig. 2, top). Once again, we see that thermal fluctuations can both accelerate the phase separation and destroy large-scale gradients in $\phi(\mathbf{r}, t)$.

B. Characterizing the length scale $R(t)$

The dynamical scaling hypothesis implies that the structure function $S(\mathbf{q}, t) = \langle\phi_{\mathbf{q}}(t)\phi_{-\mathbf{q}}(t)\rangle$ only depends on time

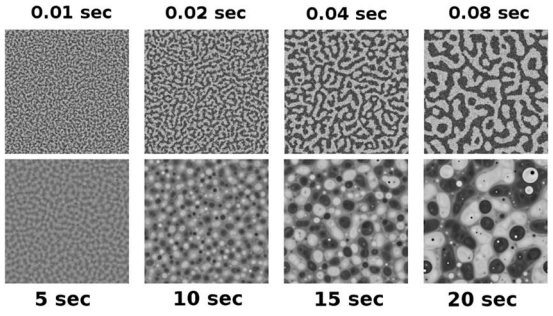

FIG. 2. If bulk diffusion is slow compared to hydrodynamic effects, the effects of thermal fluctuations are more apparent; as in the system of Fig. 1, fluctuations significantly speed up coarsening and prevent large-scale gradients in $\phi(\mathbf{r}, t)$ from forming, completely suppressing the morphology observed at $k_BT = 0$. $\eta_m = 5 \times 10^{-8}$ surface Poise (s.P., P-cm), $\eta_f = 0.01$ P, line tension $\sigma = 0.2$ pN, interface width $\xi = 20$ nm, a system size of 20 μm $\times$ 20 μm, and concentration diffusion coefficient $D_\phi = 2M\epsilon = 1.3 \times 10^{-10}$ cm^2/s. Top: $T = 21\,^\circ$C, $\Delta t = 30$ ns. Bottom: $k_BT = 0$, $\Delta t = 100$ μs.

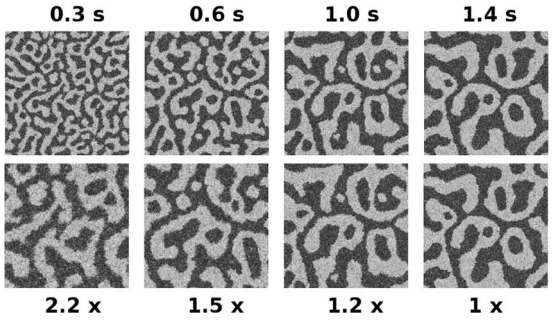

FIG. 3. Apparent dynamic scaling in the "3D viscous hydrodynamic" limit. Top: Evolution of concentration field. Bottom: Lower row images are obtained by rescaling (i.e., zooming in) and cropping the upper row images by a factor of $(1.4s/t)^{1/2}$. These images show qualitative similarity in morphology and length scale, suggesting the presence of dynamic scaling with exponent 1/2 (see text). $\eta_m = 5 \times 10^{-6}$ surface Poise (s.P., P-cm), $\eta_f = 4$ P, line tension $\sigma = 0.8$ pN, interface width $\xi = 5$ nm, and system size of 5 μm $\times$ 5 μm, and time step 4 μs, and concentration diffusion coefficient $D_\phi = 2M\epsilon = 6.5 \times 10^{-10}$ cm^2/s.

through $R(t)$ (Eq. (3)). The dynamic length scale $R(t)$ may be extracted from $S(\mathbf{q}, t)$ by taking moments of the circularly averaged structure function, $S(q, t)$,

$$R_n(t) \equiv 2\pi \left(\frac{\int dq\, q^n S(q,t)}{\int dq S(q,t)} \right)^{-1/n} \sim R(t). \qquad (5)$$

Different values of n in Eq. (5) are guaranteed to reproduce the same scaling exponent if Eq. (3) is obeyed. However, in pure 2D fluids at low Reynolds number, different moments yield different scaling exponents α_n, showing a violation of dynamic scaling.[8] Because some of these moments may not converge in general, we have applied the cutoff of Ref. 8, integrating Eq. (5) only up to $5q_{peak}$, where q_{peak} is the location of the structure function's maximum. We average over three independent runs, in addition to the angular average over each run, to construct $S(q, t)$.

C. Critical composition, $R \gg L_{sd}$ (3D viscous / 3DV)

We first consider dynamics in the asymptotic long time limit ($R(t) \gg \xi, L_{sd}$) for critical compositions ($\langle\phi\rangle = 0$, leading to bicontinuous morphologies). This limit is difficult to reach unambiguously using physical parameters and length scales fully consistent with experimental measurements. Instead, we achieve the $R(t) \gg L_{sd}$ 3D limit associated with the final phases of coarsening by choosing $\eta_f = 4$ P (400 times higher than water); this sets $L_{sd} = 6$ nm when we choose all other parameters consistent with experimental values. Equation (1) was numerically solved on a 1024 $\times$ 1024 discrete grid for an initial condition of $\phi = 0$ everywhere; the results are shown in Fig. 3 along with the full set of parameter values. These values have also been chosen to minimize residual diffusion (15%), while still preserving local equilibrium, as in Ref. 38.

For the $R(t) \gg L_{sd}$ limit of Fig. 3, we find that $R_n(t) \sim t^\alpha$ for integer and half-integer modes $-3 \le n \le 3$, with $\alpha = 0.51 \pm 0.03$ (Fig. 4).

To ensure that the scaling hypothesis is valid, we can use our scaling exponent to rescale either the concentration field (as in Ref. 7) or the structure function (as in Ref. 46). For each snapshot in the top row of Fig. 3, we rescale the image by a factor $(t_{\rm end}/t)^{1/2}$; if the dynamic scaling hypothesis is satisfied with exponent $\alpha = 1/2$, these images should be statistically similar, as they are. We can see the scaling of Eq. (3) explicitly by collapsing onto the form $g(qR) = S(q, t)/R^2(t)$, with $R(t) = (\sigma t/\eta_f)^{1/2}$, the value predicted theoretically (see Sec. II). This result is plotted in Fig. 5.

Though we see scaling at this particular set of parameters, this is not a universal feature of the system. Scaling violations have previously been shown to occur in the two-dimensional limit of our model.[7,8] Recently, Fan *et al.* have also noted that scaling is not seen in this system at zero temperature.[37] Their model is, up to numerical implementation, the $k_BT = 0$ case of our simulations in this and an earlier paper.[36]

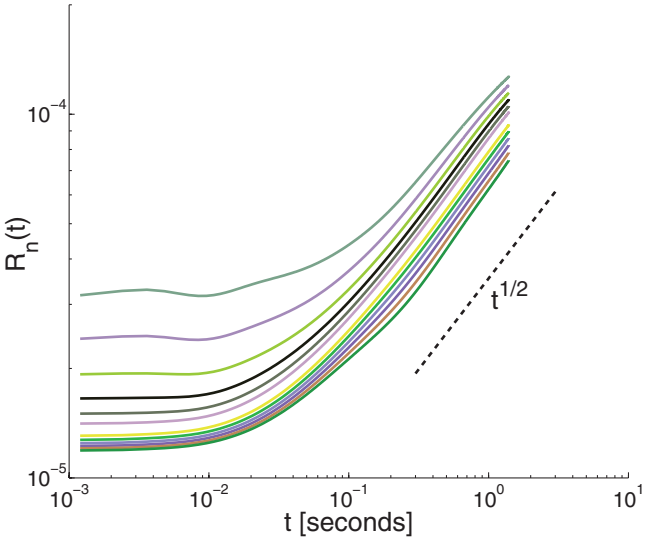

FIG. 4. In the 3D viscous limit (3DV), we see that the scaling of $R_n(t)$ is consistent with $R_n(t) \sim t^\alpha$ with $\alpha = 0.5$, with $R_n(t)$ calculated from Eq. (5). $R_n(t)$ is extracted from the structure function $S(q, t)$ evaluated from three independent simulations with the parameters of Fig. 3, as described in Sec. III B. The mean value of α is 0.51, with standard deviation 0.03. The curves in this figure have been smoothed for clarity. Different curves correspond to different values of n.

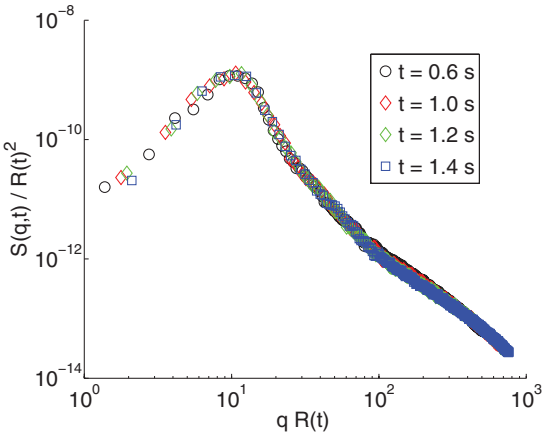

FIG. 5. The structure function $S(q, t)$ collapses onto the universal form $g(x) = S(q, t)/R(t)^2$ as a function of $x = qR(t)$ for the parameters of Fig. 3. This explicitly shows the scaling of Eq. (3) with $R(t) = (\sigma t/\eta_f)^{1/2}$.

We also observe scaling violation at zero temperature, consistent with the simulations of Fan *et al.*[37] Scaling violation is also apparent at nonzero temperatures, depending on the line tension of the system (Fig. 6). Recent experiments observe both the morphology of Figs. 3 and 6, even on identically prepared vesicles.[47] Line tensions are known to vary significantly from vesicle to vesicle, potentially due to composition differences,[48] which may explain the different morphologies observed.

Why does the membrane system of Fig. 3 display dynamical scaling while the system with larger line tension, Fig. 6, does not? Scaling violation in an ordinary two-dimensional binary fluid has been observed when isolated circular domains coarsen at a different rate than continuous, elongated ones.[7] In fact, Bray had earlier noted that the hydrodynamic term of Eq. (1) should vanish for a single spherical droplet in the absence of noise.[1] This basic fact implies that droplets will not merge at a sufficiently fast rate to keep up with the bicontinuous phase, leading to morphologies such that of Fig. 6.

In the system with lower line tension, Fig. 3, we observe that these domains merge and coalesce, rather than remaining isolated. We believe that this is related to the presence of thermal fluctuations, as scaling is never observed in the zero-temperature 3DV limit, either in our simulations or in those of Fan *et al.*[37] As discussed earlier, thermal coalescence provides an additional mechanism for the coarsening of isolated domains. In addition, scaling violation is observed as the line tension is increased. Making the line tension larger has two immediate effects: it increases the speed of line tension driven coarsening relative to coarsening due to thermal coalescence, and it suppresses fluctuations of domain boundaries. Both effects reduce the importance of thermal noise. Our renormalization group arguments suggest that temperature should be irrelevant at long times, but our simulations show that thermal noise may create very good apparent scaling.

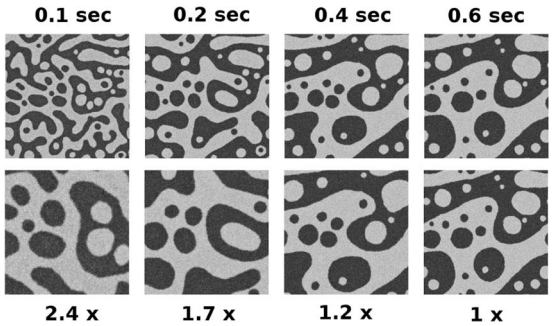

FIG. 6. If the line tension is increased, reducing the influence of thermal fluctuations, scaling violation may be observed in the "3D viscous hydrodynamic limit," as opposed to the apparent scaling of Fig. 3. Top: Evolution of concentration field. Bottom: Rescaling with exponent 1/2 shows scaling violation. $\eta_m = 5 \times 10^{-6}$ surface Poise (s.P., P-cm), $\eta_f = 4$ P, line tension $\sigma = 4$ pN, interface width $\xi = 5$ nm, and system size of 5 μm $\times$ 5 μm, and time step 2 μs, and concentration diffusion coefficient $D_\phi = 2M\epsilon = 6.5 \times 10^{-10}$ cm^2/s. $T = 21\,^\circ$C ($k_BT = 4.061$ pN nm).

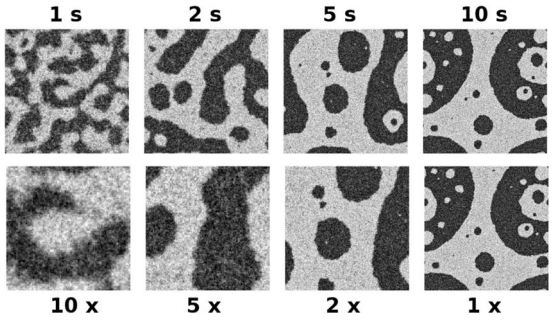

FIG. 7. Scaling is violated in pure two-dimensional systems. Top: Evolution of concentration field. Morphological changes show scaling violation. Bottom: Rescaling with $\alpha = 1$ shows scaling is absent (see text). $\eta_m = 5 \times 10^{-6}$ s.P., $\eta_f = 0$, line tension $\sigma = 0.1$ pN, interface width $\xi = 40$ nm, and system size of 30 μm $\times$ 30 μm, and time step 10 μs. The concentration diffusion coefficient $D_\phi = 2M\epsilon = 6.5 \times 10^{-10}$ cm^2/s. $T = 21\,^\circ$C ($k_BT = 4.061$ pN nm).

D. Critical composition, $R \ll L_{sd}$ (2D viscous / 2DV)

Lowering the bulk viscosity but maintaining critical concentrations leads to a violation of scaling, as for a pure 2D fluid (Fig. 7). In these cases, the absence of scaling is clear, as morphological changes between continuous structure and isolated domains are observed. This is made evident by attempting to rescale the concentration field by using the exponent $\alpha_1 \approx 1$ (Fig. 7, bottom). Similar morphological changes are observed experimentally in phase-separating giant unilamellar vesicles.[29] Fitting $R_n(t)$ to the form t^{α_n}, we find α_n to vary between 0.8 and 1.2 for $n =$ integers and half integers from -3 to 3. This also provides supporting evidence for the breakdown of dynamical scaling, as we would expect α_n to be independent of n if Eq. (3) holds. The variation in α_n here differs from the errors reported in Table I, which also include statistical errors and systematic errors in α from changing the fitting range.

E. Off-critical coalescence, $R \gg L_{sd}$ (3D coalescence / 3DC)

For an off-critical system, $\langle\phi\rangle \neq 0$, at length scales above the Saffman-Delbrück length ($R(t) \gg L_{sd}$) we expect that thermally driven domain coalescence will drive coarsening if $k_BT \gg \sigma M \eta_f$. We simulate a system with η_f chosen to be large

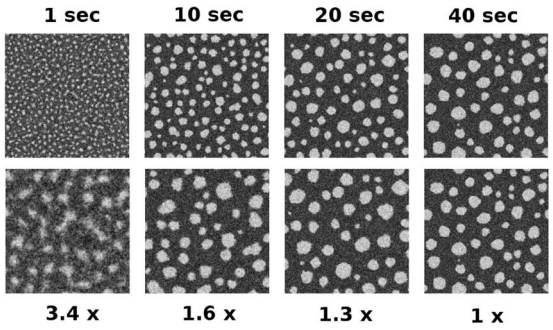

FIG. 8. Thermally driven coalescence leads to scaling with exponent 1/3 for $R \gg L_{sd}$. Top: Evolution of concentration field. Bottom: Rescaling with $\alpha = 1/3$ shows dynamical scaling for all but the shortest times. $\eta_m = 5 \times 10^{-6}$ s.P., $\eta_f = 5$ P, line tension $\sigma = 0.4$ pN, interface width $\xi = 15$ nm, and system size of 10 μm $\times$ 10 μm, and time step 25 μs. $D_\phi = 1.3 \times 10^{-10}$ cm^2/s. $\langle\phi\rangle = -0.2$. $T = 21\,^\circ$C ($k_BT = 4.061$ pN nm).

enough that L_{sd} is small compared to the interface width. We also ensure that $k_BT/\sigma M\eta_f \approx 300$ is large, placing us clearly in the coalescence region (Table I). We can observe visually that domain diffusion and coalescence is the primary source of coarsening (Fig. 8). We also observe scaling with the predicted exponent of 1/3 (Figs. 8 and 9), though the uncertainty on this exponent is large (Table I). We note that the predicted theoretical exponent has been derived in the context of sharp-interface theories, and if this limit is not appropriate to the phase field simulations, other results may be possible.[45]

F. Off-critical coalescence, $R \ll L_{sd}$ (2D coalescence / 2DC)

Below the Saffman-Delbrück length ($R(t) \ll L_{sd}$), domain diffusion coefficients scale logarithmically with domain size, and we expect domain coalescence to dominate for length scales $R(t)$ larger than $\eta_m M\sigma/k_BT$. We simulate a system in the pure two-dimensional limit, $\eta_f = 0$, with $\eta_m M\sigma/k_BT = 0.5$ nm, placing us in the 2D coalescence regime. Domain diffusion and coalescence is the primary source of coarsening (Fig. 10). The predicted exponent of 1/2 is observed (Figs. 10 and 11).

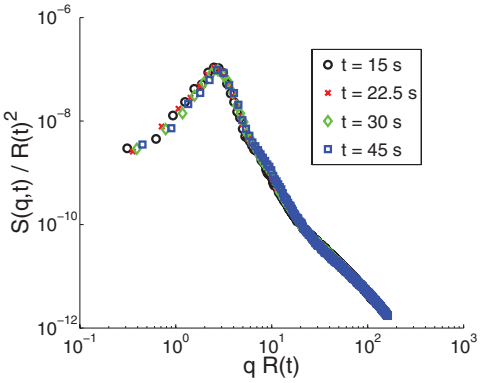

FIG. 9. Collapse plot of $g(x) = S(q, t)/R(t)^2$ as a function of $x = qR(t)$ explicitly shows the scaling of Eq. (3) with $R(t) = (k_BTt/\eta_f)^{1/3}$. Data correspond to the same simulations as in Fig. 8.

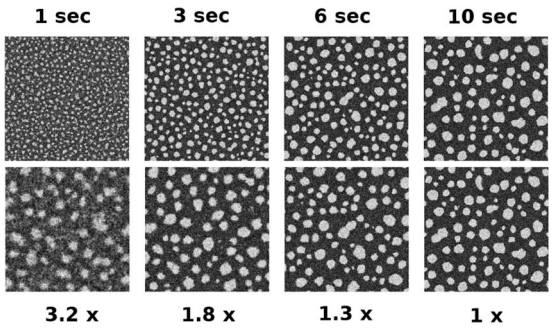

FIG. 10. Thermally driven coalescence leads to scaling with exponent 1/2 for $R \ll L_{sd}$. Top: Evolution of concentration field in 2D coalescence limit. Bottom: Rescaling with $\alpha = 1/2$ shows dynamical scaling for all but the shortest times. $\eta_m = 5 \times 10^{-6}$ s.P., $\eta_f = 0$, line tension $\sigma = 0.1$ pN, interface width $\xi = 40$ nm, and system size of 10 μm $\times$ 10 μm, and timestep 5 μs. $D_\phi = 6.5 \times 10^{-10}$ cm^2/s. $T = 21^\circ$C ($k_BT = 4.061$ pN nm). $\langle\phi\rangle = -0.2$.

G. Barely off-critical systems

In a system barely off the critical 50% area fraction, an initial bicontinuous structure will form, but this pattern is unstable, and will break down into isolated domains (Fig. 12). This is a particularly relevant issue for experiments, as different vesicles prepared identically may have compositions differing by a few percent.[29,48]

IV. RELATION TO EXPERIMENTS AND OTHER SIMULATIONS

Coarsening has been directly measured in off-critical multicomponent lipid vesicles,[31,32] with results for the coarsening exponent varying between $R \sim t^{0.15}$ and $R \sim t^{2/3}$. We argue that these experiments may not be probing a single scaling regime. We first determine the likely regimes of these experiments. In real membranes, M and η_m are coupled, as $D_\phi = 2M\epsilon \approx k_BT/(4\pi\eta_m)$. Applying this result and determining ϵ from typical line tensions ($\sigma \sim 0.1$ pN) interface widths ($\xi \sim 10$ nm) and compositions ($\phi_0 \approx 0.4$) as in Ref. 36, sets $\sqrt{M\eta_m}$, $M\eta_f < 10$ nm, suggesting that experiments fall well outside the Cahn-Hilliard regime. This is consistent with

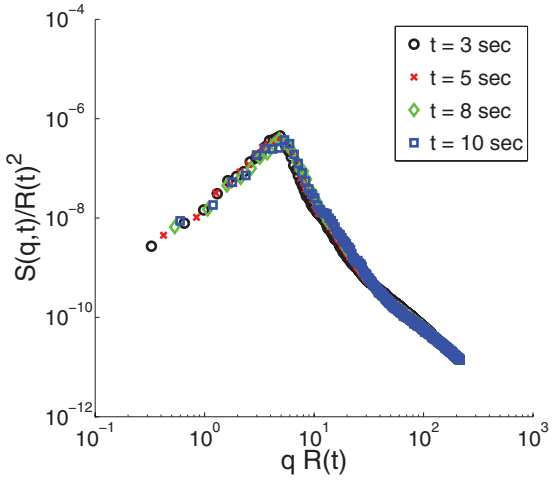

FIG. 11. Collapse plot of $g(x) = S(q, t)/R(t)^2$ as a function of $x = qR(t)$ explicitly shows the scaling of Eq. (3) with $R(t) = (k_BTt/\eta_m)^{1/2}$. Data correspond to the same simulations as in Fig. 10.

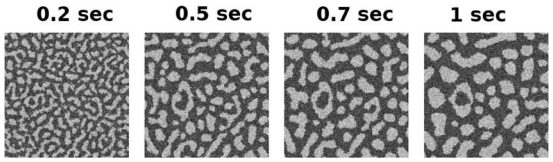

FIG. 12. If the composition is not precisely at the critical area fraction, the bicontinous structure is unstable to the formation of domains. $\eta_m = 5 \times 10^{-6}$ surface Poise (s.P., P-cm), $\eta_f = 4$ P, line tension $\sigma = 4$ pN, interface width $\xi = 5$ nm, and system size of 5 μm $\times$ 5 μm, and time step 2 μs, and concentration diffusion coefficient $D_\phi = 2M\epsilon = 6.5 \times 10^{-10}$ cm^2/s. $T = 21\,^\circ$C ($k_BT = 4.061$ pN nm). $\langle\phi\rangle = -0.05$, corresponding to a 56-44 mix.

experimental results that report coalescence, not ripening.[29,32] In standard model membranes, η_m lies in the range of $0.1 \times 10^{-6} - 10 \times 10^{-6}$ surface poise (P-cm, or g/s),[17,49,50] corresponding to $L_{sd} \sim 0.1 - 10$ μm. Micron-scale domains measured in Refs. 31 and 32 are likely to be intermediate between the regimes of 2D and 3D coalescence, and these experiments may not measure a common scaling exponent.

We emphasize that without characterization of (at the least) membrane viscosity, coarsening measurements on membranes are not readily interpreted; apparent values of α from our simulations when outside of a clear scaling limit have ranged from 0.2 to 1.2. The 3D regime ($L_{sd} \ll R(t) \ll R_{vesicle}$) may be enlarged by increasing solution viscosity, thereby decreasing L_{sd}, or by increasing vesicle radii. This would ensure that experimental measurements are observing a single well-defined regime.

Experiments measuring coarsening in supported membranes report an off-critical-mixture exponent of $\alpha = 0.31$.[33] Our scaling results are readily generalized to such a case. For membranes separated from a wall by a thin layer of fluid of size $h \ll L_{sd}$, $T^m(r) \sim 1/r^2$ for large r,[24,51] and scaling theory gives $\alpha = 1/3$ for both diffusive and hydrodynamic coarsening, but $\alpha = 1/4$ for the coalescence mechanism (this is discussed in greater detail below).

Previous simulations using dissipative particle dynamics have also reported $R(t) \sim t^{1/2}$ for critical mixtures, $R(t) \sim t^{1/3}$ for off-critical;[34] other dissipative particle dynamics simulations report $t^{1/3}$ for both critical and off-critical scaling.[35] Our theory explains the inconsistency between these two results as a result of the two simulations being in different regimes (Table I). Both models have similar line tensions ($\sim$10 pN) and explore the range $R \gg L_{sd}$, but the model of Ramachandran *et al.*[35] represents lipids as single particles, while the model of Laradji and Kumar[34] includes a more realistic representation of lipid structure, and likely has an increased membrane viscosity and decreased mobility M relative to that of Ref. 35. In our simulations, decreasing M by a factor of 20 can change the scaling exponent from $\alpha \sim 1/3$ (3D Cahn-Hilliard regime) to $\alpha \sim 1/2$ (3D viscous regime).

V. SIMPLE GENERALIZATIONS

Our simulation and scaling theory both admit some very simple generalizations. The hydrodynamics of a supported lipid membrane are well-understood, and lead to versions of the membrane Oseen tensor (Eq. (2)) that have long-distance dependence of r^{-1} or r^{-2}, depending on the distance between the membrane and the substrate.[51] In the "free far" region where the Oseen tensor has an r^{-1} dependence, the coarsening kinetics should be essentially the same as our 3D viscous regime. However, in the "adsorbed" and "supported hovering" limits, where $T(r) \sim r^{-2}$, our dimensional analysis arguments give $\alpha = 1/3$ for both diffusive (LSW) and hydrodynamic coarsening (i.e., the viscosity of the bulk fluid is a marginal variable). Diffusion coefficients $D(R) \sim R^{-2}$ for objects in a supported membrane in this limit;[51,52] setting $D(R)t \sim R(t)^2$ gives $\alpha = 1/4$ for the coalescence mechanism. These results are identical to those for coarsening in a Hele-Shaw cell,[1] as the supported membrane Oseen tensor naturally reduces to the Hele-Shaw result when the drag from the substrate is large.

While dynamical scaling breaks down in two-dimensional fluids in the viscous limit, it is restored in the inertial limit.[8,9] Though the Reynolds number of flows in membranes is generally small,[10] and thus we generally expect inertial effects to be negligible, it may be interesting to explore phase separation in this limit. We can derive a generalized, frequency-dependent Oseen tensor that includes the effects of inertia,[15]

$$T^{ij}_{\text{inertial}}(\mathbf{k}, \omega) = \frac{\delta_{ij} - k_i k_j/k^2}{i\omega\rho_m + \eta_m k^2 + 2\eta_f k\sqrt{1 + i\omega/\omega_f(k)}}, \tag{6}$$

where ρ_m is the two-dimensional membrane mass density, ρ_f the bulk fluid density, and $\omega_f(k) = \eta_f k^2/\rho_f$. The equation of motion for the membrane velocity is then

$$v_i(\mathbf{k}, \omega) = T^{ij}_{\text{inertial}}(\mathbf{k}, \omega) f_j(\mathbf{k}, \omega), \tag{7}$$

where $\mathbf{f}$ is the force applied to the membrane, $\mathbf{f}(\mathbf{r}, t) = \frac{\delta H}{\delta \phi}\nabla\phi + \zeta$. Our convention is $\mathbf{f}(\mathbf{k}, \omega) = \int d^2r dt e^{-i(\mathbf{k}\cdot\mathbf{r} + \omega t)}\mathbf{f}(\mathbf{r}, t)$. We can apply our scaling estimates to these equations, with $k \sim 1/R(t)$, $\omega \sim 1/t$. We also note that $v(\mathbf{k}, \omega) \sim (R(t)^2 t)\, v(\mathbf{r}, t) \sim R(t)^3$. If the dominant contribution to the Oseen tensor is from the two-dimensional membrane density ρ_m, we find that $R(t) \sim t^{2/3}$, which is just the usual two-dimensional inertial scaling.[1,8] However, if the dominant contribution is from the *three-dimensional* mass density ρ_f, we find $R(t) \sim t^{1/2}$. We expect this to be the dominant asymptotic scaling if inertia is relevant; we note that at long times, momentum transport through the outside fluid dominates the velocity autocorrelation function.[15] Inertial simulations using Eq. (6) as a basis may also be possible. However, if the velocity of the outside fluid is a true dynamical variable, eliminating it from our description will cause the dynamics to be non-Markovian,[14] and full three-dimensional hydrodynamic simulations may be more appropriate.

VI. CONCLUSIONS

We have applied simple scaling theories to predict the behavior of phase-separating multicomponent membranes, and compared these results to continuum hydrodynamic simulations. Theory and simulation show that both the morphology and the scaling exponent will depend on the relative importance of diffusion, hydrodynamics, and thermal

fluctuations. We present different scaling regimes where each of these effects dominate. One feature unique to the membrane system is the appearance of an additional hydrodynamic length scale, the Saffman-Delbrück length L_{sd}; domains will coarsen with different morphologies and exponents depending on whether they are smaller or larger than L_{sd} (the "2D" and "3D" limits, respectively). Scaling theories correctly describe the dynamical scaling exponents in the regions of parameter space where the phase separation mechanism is bulk diffusion, evaporation-condensation, and thermal coalescence, but fail to predict the observed scaling violation in the critical ($\langle\phi\rangle = 0$) viscous limits. In addition to the violation of scaling for bicontinuous phase separation both in the 2D and 3D limits we observe a region of apparent scaling in the 3D regime, with scaling exponent 1/2; this scaling is connected to the presence of thermal fluctuations, and can be suppressed by increasing the line tension. We apply our scaling results to analyze experiments and other simulations that attempt to measure the scaling exponent, and suggest that the measurement of the membrane viscosity is a necessary prerequisite for understanding these results. We also apply our scaling theory to predict how the scaling exponent will change if the experimental conditions are modified, such as treating a supported membrane.

ACKNOWLEDGMENTS

This work was supported in part by the National Science Foundation (NSF) (Grant Nos. CHE-0848809, CHE-032168, and CNS-0960316) and the BSF (Grant No. 2006285). F.L.H.B. is a Camille Dreyfus Teacher-Scholar. B.A.C. acknowledges the support of the Fannie and John Hertz Foundation. We also thank Haim Diamant, Mikko Haataja, Sarah Keller, and Cynthia Stanich for useful discussions.

APPENDIX: FLUCTUATION-DISSIPATION AND THE NONINERTIAL LIMIT

Our model describes composition dynamics via a nonlinear Langevin equation, Eq. (1). We chose this model by analogy with the noninertial limit of model H dynamics for a binary fluid.[53] This limit has been applied to analytic studies of phase separation,[1,54] and has been numerically evaluated at $k_BT = 0$,[46] but a subtle issue appears in the numerical evolution of our Langevin equation at finite temperature. Equations (1) and (2) has a multiplicative noise term, which admits multiple interpretations.[55] We show in this section that the Stratonovich interpretation of our equations of motion is necessary in order to obey fluctuation-dissipation, and have the Boltzmann distribution as the steady state distribution.

1. Preliminaries

Our equations of motion for both the lipid composition $\phi(\mathbf{r}, t)$ consist of nonlinear Langevin equations with multiplicative noise. This sort of equation can be written in the form

$$\frac{\partial z_i(t)}{\partial t} = A_i(\mathbf{z}) + B_{ij}(\mathbf{z})R_j(t), \tag{A1}$$

where we have assumed the Einstein summation convention; we will assume this convention throughout for Latin indices, but will explicitly note sums over momenta ($\mathbf{q}$, $\mathbf{p}$, etc.). Here, $R_j(t)$ is a Gaussian Langevin noise with zero mean and variance,

$$\langle R_i(t)R_j(t')\rangle = \delta_{ij}\delta(t-t'). \tag{A2}$$

However, if B_{ij} depends on $\mathbf{z}$, Eq. (A1) is susceptible to different interpretations and needs to be supplemented with additional information.[55] There are two distinct interpretations: Ito and Stratonovich, which are most easily distinguished by the Fokker-Planck equation corresponding to Eq. (A1). In the Ito convention, the Fokker-Planck equation for Eq. (A1) is

$$\frac{\partial P}{\partial t} = -\frac{\partial}{\partial z_i}[A_i P] + \frac{1}{2}\frac{\partial}{\partial z_i}\frac{\partial}{\partial z_j}[B_{ik}(\mathbf{z})B_{jk}(\mathbf{z})P] \quad \text{(Ito)}, \tag{A3}$$

where P is the conditional probability density $P = P(\mathbf{z}, t|\mathbf{z}_0, t_0)$. By contrast, in the Stratonovich interpretation, Eq. (A1) is equivalent to

$$\frac{\partial P}{\partial t} = -\frac{\partial}{\partial z_i}[A_i P] + \frac{1}{2}\frac{\partial}{\partial z_i} \times \left\{B_{ik}(\mathbf{z})\frac{\partial}{\partial z_j}[B_{jk}(\mathbf{z})P]\right\} \quad \text{(Stratonovich)}. \tag{A4}$$

From this, we can see that the Stratonovich interpretation of Eq. (A1) is equivalent to an Ito equation with a modified drift term,

$$A_i^{\text{Ito}} = A_i^{\text{Strat}} + \frac{1}{2}B_{jk}\frac{\partial}{\partial z_j}B_{ik}. \tag{A5}$$

One particularly useful special case of the general Langevin equation Eq. (A1) is one where the drift term is derived from an energy H,

$$\frac{\partial z_i(t)}{\partial t} = -M_{ij}(\mathbf{z})\frac{\partial H}{\partial z_j} + B_{ij}(\mathbf{z})R_j(t). \tag{A6}$$

The well-known "Brownian dynamics with hydrodynamic interactions" algorithm[56] takes on a version of this form, and we will see that our membrane composition simulation does as well. If we choose the Stratonovich interpretation, the Fokker-Planck equation corresponding to Eq. (A6) is

$$\frac{\partial P}{\partial t} = \frac{\partial}{\partial z_i}\left[\left(M_{ij}(\mathbf{z})\frac{\partial H}{\partial z_j} - \frac{1}{2}B_{jk}\frac{\partial}{\partial z_j}B_{ik}\right)P\right] + \frac{1}{2}\frac{\partial}{\partial z_i}\frac{\partial}{\partial z_j}\left[B_{ik}(\mathbf{z})B_{jk}(\mathbf{z})P\right] \quad \text{(Stratonovich)}. \tag{A7}$$

If the fluctuation-dissipation relationship $B_{ik}B_{jk} = 2k_BTM_{ij}$ holds, and $B_{jk}\frac{\partial}{\partial z_j}B_{ik} = k_BT\frac{\partial M_{ij}}{\partial z_j}$, it is simple to see that the equilibrium distribution $P \sim \exp(-H/k_BT)$ will be a steady state of Eq. (A7).

If we choose the Ito interpretation, the Fokker-Planck equation corresponding to Eq. (A6) is

$$\frac{\partial P}{\partial t} = \frac{\partial}{\partial z_i}\left[\left(M_{ij}(\mathbf{z})\frac{\partial H}{\partial z_j}\right)P\right] + \frac{1}{2}\frac{\partial}{\partial z_i}\frac{\partial}{\partial z_j}\left[B_{ik}(\mathbf{z})B_{jk}(\mathbf{z})P\right] \text{ (Ito)}. \quad \text{(A8)}$$

In the Ito case, the Boltzmann distribution will be the steady state of Eq. (A8) if the fluctuation-dissipation relationship $B_{ik}B_{jk} = 2k_BTM_{ij}$ holds, and $k_BT\frac{\partial M_{ij}}{\partial z_j} = 0$.

2. Membrane composition dynamics

Our overdamped model H for simulations of phase separation in a model membrane is given by

$$(\partial_t + \mathbf{v}\cdot\nabla)\phi(\mathbf{r},t) = M\nabla^2\frac{\delta H}{\delta\phi(\mathbf{r},t)} + \theta(\mathbf{r},t), \quad \text{(A9)}$$

$$v_i(\mathbf{r},t) = \int d^2r'\, T^m_{ij}(\mathbf{r}-\mathbf{r}')\left[\frac{\delta H}{\delta\phi(\mathbf{r}',t)}\nabla'_j\phi(\mathbf{r}',t) + \zeta_j(\mathbf{r}',t)\right]. \quad \text{(A10)}$$

where the continuum Fourier transform of T^m_{ij} is[11,24]

$$T^m_{ij}(\mathbf{q}) = \int d^2r\, T^m_{ij}(\mathbf{r})e^{-i\mathbf{q}\cdot\mathbf{r}} = \frac{1}{\eta_m(q^2 + q/L_{sd})}\left(\delta_{ij} - \frac{q_iq_j}{q^2}\right), \quad \text{(A11)}$$

where the integral is over all space. We note that $q_iT^m_{ij}(\mathbf{q}) = 0$ as a result of the incompressibility constraint $\nabla\cdot\mathbf{v}_m = 0$ on the membrane. We will use $T^{ij}_{\mathbf{k}}$ as a shorthand for $T^m_{ij}(\mathbf{k})$.

In Fourier space, these equations are

$$\partial_t\phi_{\mathbf{q}}(t) + \{\mathbf{v}\cdot\nabla\phi(\mathbf{r},t)\}_{\mathbf{q}} = -Mq^2\left\{\frac{\delta H}{\delta\phi(\mathbf{r},t)}\right\}_{\mathbf{q}} + \theta_{\mathbf{q}}, \quad \text{(A12)}$$

$$v_{\mathbf{q},i}(t) = T^m_{ij}(\mathbf{q})\left\{\frac{\delta H}{\delta\phi(\mathbf{r},t)}\nabla_j\phi(\mathbf{r},t) + \zeta_j\right\}_{\mathbf{q}}, \quad \text{(A13)}$$

where $\{f(\mathbf{r})\}_{\mathbf{q}}$ is the Fourier component of $f(\mathbf{r})$. The Fourier conventions we use are $\phi_{\mathbf{q}} = \int_{\mathcal{L}} d^2r\,\phi(\mathbf{r})e^{-i\mathbf{q}\cdot\mathbf{r}}$, and $\phi(\mathbf{r}) = \mathcal{L}^{-2}\sum_q \phi_{\mathbf{q}}e^{i\mathbf{q}\cdot\mathbf{r}}$. The variances of the Langevin forces are

$$\langle\theta_{\mathbf{q}}(t)\theta_{\mathbf{q}'}(t')\rangle = 2k_BTMq^2\mathcal{L}^2\delta_{\mathbf{q},-\mathbf{q}'}\delta(t-t'), \quad \text{(A14)}$$

$$\langle\zeta_{\mathbf{q},i}(t)\zeta_{\mathbf{q}',j}(t')\rangle = 2k_BT\mathcal{L}^2\eta_m(q^2 + q/L_{sd})\delta_{ij}\delta_{\mathbf{q},-\mathbf{q}'}\delta(t-t'). \quad \text{(A15)}$$

We want to show that the Langevin equations, Eqs. (A12)–(A15), drive the system to the Boltzmann distribution, $\sim e^{-H/k_BT}$. The difficult term in this calculation is the velocity term, which has multiplicative noise. For simplicity, we take $M = 0$, ignoring the bulk diffusion term for now. Then our Langevin equations become, writing out the Fourier transform of $\mathbf{v}\cdot\nabla\phi$ explicitly as a convolution,

$$\partial_t\phi_{\mathbf{q}}(t) = -\frac{1}{\mathcal{L}^2}\sum_{\mathbf{k}} v^i_{\mathbf{k}}\sqrt{-1}(q-k)^i\phi_{\mathbf{q}-\mathbf{k}}, \quad \text{(A16)}$$

where $v^i_{\mathbf{k}} = T^{ij}_{\mathbf{k}}f^{\text{comp}}_j(\mathbf{k})$, and $f^{\text{comp}}_j(\mathbf{k}) = \{\frac{\delta H}{\delta\phi(\mathbf{r},t)}\nabla_j\phi(\mathbf{r},t) + \zeta_j\}_{\mathbf{k}}$. We note that in our convention, $\{\frac{\delta H}{\delta\phi(\mathbf{r})}\}_{\mathbf{k}} = \mathcal{L}^2\frac{\partial H}{\partial\phi_{-\mathbf{k}}}$. In Eq. (A16) and below, upper indices refer to the vector or tensor component; no exponentiation is implied. This force can be written explicitly in Fourier space by using the convolution theorem,

$$f^{\text{comp}}_j(\mathbf{k}) = \sum_{\mathbf{p}}\left[\frac{\partial H}{\partial\phi_{-\mathbf{p}}}\sqrt{-1}(k-p)^j\phi_{\mathbf{k}-\mathbf{p}}\right] + r_kR_j(\mathbf{k}), \quad \text{(A17)}$$

where $r_k = \left[2k_BT\mathcal{L}^2\eta_m(k^2 + k/L_{sd})\right]^{1/2}$ and $R_j(\mathbf{k})$ is a Langevin force with $\langle R_i(\mathbf{k},t)R_j(\mathbf{k}',t')\rangle = \delta_{ij}\delta_{\mathbf{k},-\mathbf{k}'}\delta(t-t')$.

Our Langevin equation, Eq. (A16), is now in the form

$$\partial_t\phi_{\mathbf{q}} = -\sum_{\mathbf{p}} M(\mathbf{q},\mathbf{p})\frac{\partial H}{\partial\phi_{\mathbf{p}}} + \sum_{\mathbf{p}} B(\mathbf{q},\mathbf{p})R(\mathbf{p}), \quad \text{(A18)}$$

where

$$M(\mathbf{q},\mathbf{p}) = -\frac{1}{\mathcal{L}^2}\sum_{\mathbf{k}}(q-k)^i\phi_{\mathbf{q}-\mathbf{k}}T^{ij}_{\mathbf{k}}(k+p)^j\phi_{\mathbf{k}+\mathbf{p}}, \quad \text{(A19)}$$

$$B(\mathbf{q},\mathbf{p}) = -\frac{1}{\mathcal{L}^2}\sqrt{-1}(q-p)^i\phi_{\mathbf{q}-\mathbf{p}}T^{ij}_{\mathbf{p}}r_p. \quad \text{(A20)}$$

We have suppressed a vector index on $B(\mathbf{q},\{\mathbf{p},j\})$ and $R_j(\mathbf{p})$ for simplicity; the sum over j is implied. The Langevin equation. Eq. (A18) is in the form of Eq. (A6), though we have written out the sum over $\mathbf{p}$ explicitly.

The Fokker-Planck equation corresponding to our Langevin equation, Eq. (A18), is (in the Stratonovich interpretation)

$$\frac{\partial P}{\partial t} = \sum_{\mathbf{q},\mathbf{p}}\frac{\partial}{\partial\phi_{\mathbf{q}}} \times\left[\left(M(\mathbf{q},\mathbf{p})\frac{\partial H}{\partial\phi_{\mathbf{p}}} - \frac{1}{2}\sum_{\mathbf{k},\mathbf{p}}B(\mathbf{p},-\mathbf{k})\frac{\partial}{\partial\phi_{\mathbf{p}}}B(\mathbf{q},\mathbf{k})\right)P\right] + \frac{1}{2}\sum_{\mathbf{q},\mathbf{p}}\frac{\partial}{\partial\phi_{\mathbf{q}}}\frac{\partial}{\partial\phi_{\mathbf{p}}}\left(\sum_{\mathbf{k}}B(\mathbf{q},\mathbf{k})B(\mathbf{p},-\mathbf{k})P\right).$$

The slight difference between this result and that of Eq. (A4) is a result of the minor change in convention in the correlation of $R_i(\mathbf{k})$.[57] We now show that the Stratonovich interpretation of this equation has the Boltzmann distribution as a steady state; this requires us to demonstrate that $\sum_{\mathbf{k}}B(\mathbf{q},\mathbf{k})B(\mathbf{p},-\mathbf{k}) = 2k_BTM(\mathbf{q},\mathbf{p})$ and that $k_BT\sum_{\mathbf{p}}\frac{\partial}{\partial\phi_{\mathbf{p}}}M(\mathbf{q},\mathbf{p}) = 1/2\sum_{\mathbf{k},\mathbf{p}}B(\mathbf{p},-\mathbf{k})\frac{\partial}{\partial\phi_{\mathbf{p}}}B(\mathbf{q},\mathbf{k})$.

We can evaluate $\sum_{\mathbf{k}}B(\mathbf{q},\mathbf{k})B(\mathbf{p},-\mathbf{k})$,

$$\sum_{\mathbf{k}}B(\mathbf{q},\mathbf{k})B(\mathbf{p},-\mathbf{k}) = -\frac{1}{\mathcal{L}^4}\sum_{\mathbf{k}}(q-k)^i\phi_{\mathbf{q}-\mathbf{k}}(p+k)^l \times\phi_{\mathbf{p}+\mathbf{k}}T^{ij}_{\mathbf{k}}T^{jl}_{\mathbf{k}}r_k^2, \quad \text{(A21)}$$

where we have used $T^{ij}_{\mathbf{k}} = T^{ji}_{\mathbf{k}}$, $T^{ij}_{-\mathbf{k}} = T^{ij}_{\mathbf{k}}$. We note that $T^{ij}_{\mathbf{k}}$ is just proportional to the transverse projector $\wp^{ij}_{\perp}(\mathbf{k}) = (\delta_{ij} - k_i k_j/k^2)$, and that $\wp^2_{\perp} = \wp_{\perp}$, so we find $T^{ij}_{\mathbf{k}} T^{jl}_{\mathbf{k}} r_k^2 = 2k_B T \mathcal{L}^2 T^{il}_{\mathbf{k}}$. Therefore,

$$\begin{aligned}\sum_{\mathbf{k}} B(\mathbf{q},\mathbf{k})B(\mathbf{p},-\mathbf{k}) &= -\frac{2k_BT}{\mathcal{L}^2}\sum_{\mathbf{k}}(q-k)^i\phi_{\mathbf{q}-\mathbf{k}}(p+k)^l\phi_{\mathbf{p}+\mathbf{k}}T^{il}_{\mathbf{k}} \\ &= 2k_BTM(\mathbf{q},\mathbf{p}),\end{aligned} \tag{A22}$$

To check the second requirement, we note that as $\sum_{\mathbf{k}} B(\mathbf{q},\mathbf{k})B(\mathbf{p},-\mathbf{k}) = 2k_BTM(\mathbf{q},\mathbf{p})$, then $k_BT\frac{\partial}{\partial\phi_{\mathbf{p}}}M(\mathbf{q},\mathbf{p}) = \frac{1}{2}\sum_{\mathbf{k},\mathbf{p}} B(\mathbf{p},-\mathbf{k})\frac{\partial}{\partial\phi_{\mathbf{p}}}B(\mathbf{q},\mathbf{k})$ only if $\sum_{\mathbf{k},\mathbf{p}} B(\mathbf{q},\mathbf{k})\frac{\partial}{\partial\phi_{\mathbf{p}}}B(\mathbf{p},-\mathbf{k}) = 0$. We can calculate this term simply,

$$\begin{aligned}\sum_{\mathbf{k},\mathbf{p}} B(\mathbf{q},\mathbf{k})\frac{\partial}{\partial\phi_{\mathbf{p}}}B(\mathbf{p},-\mathbf{k}) &= -\frac{2k_BT}{\mathcal{L}^2}\sum_{\mathbf{k},\mathbf{p}}(q-k)^i\phi_{\mathbf{q}-\mathbf{k}}(p+k)^l\frac{\partial\phi_{\mathbf{p}+\mathbf{k}}}{\partial\phi_{\mathbf{p}}}T^{il}_{\mathbf{k}} \\ &= -\frac{2k_BT}{\mathcal{L}^2}q^i\phi_{\mathbf{q}}T^{il}_0\sum_{\mathbf{p}}p^l,\end{aligned} \tag{A23}$$

which is obviously seen to be zero by taking $\mathbf{p} \to -\mathbf{p}$. The $k = 0$ zero mode of the Oseen tensor is, in principle, infinite, but in fact is limited by the finite extent of the system, as in Ref. 58; in our simulations we only sum over $k \neq 0$, as in Ref. 59.

This derivation shows that the Stratonovich interpretation of our dynamical equations will lead to the correct Boltzmann distribution as the steady state. We can also immediately see that the Ito interpretation is not correct. If Eq. (A18) were interpreted in the Ito sense, we would require that $\sum_{\mathbf{p}}\frac{\partial}{\partial\phi_{\mathbf{p}}}M(\mathbf{q},\mathbf{p}) = 0$ in order to have the correct steady state, and this is not the case.

[1] A. J. Bray, Adv. Phys. **43**, 357 (1994).
[2] J. S. Langer, *Solids far from Equilibrium* (Cambridge University Press, Cambridge, England, 1992), p. 297.
[3] K. Binder, S. Puri, S. K. Das, and J. Horbach, J. Stat. Phys. **138**, 51 (2010).
[4] N. Goldenfeld, *Lectures on Phase Transitions and the Renormalization Group*, Frontiers in Physics (Westview Press, Boulder, CO, 1992).
[5] P. M. Chaikin and T. C. Lubensky, *Principles of Condensed Matter Physics* (Cambridge University Press, Cambridge, England, 2000).
[6] E. D. Siggia, Phys. Rev. A **20**, 595 (1979).
[7] A. J. Wagner and J. Yeomans, Phys. Rev. Lett. **80**, 1429 (1998).
[8] H. Furukawa, Phy. Rev. E **61**, 1423 (2000).
[9] A. J. Wagner and M. E. Cates, Europhys. Lett. **56**, 556 (2001).
[10] P. G. Saffman and M. Delbrück, Proc. Natl. Acad. Sci. U.S.A. **72**, 3111 (1975).
[11] N. Oppenheimer and H. Diamant, Biophys. J. **96**, 3041 (2009).
[12] J. Happel and H. Brenner, *Low Reynolds Number Hydrodynamics* (Kluwer, The Hague, 1983).
[13] J.-P. Hansen and I. R. McDonald, *Theory of Simple Liquids*, 3rd ed. (Academic, The Netherlands, 2006).
[14] R. Zwanzig, *Nonequilibrium Statistical Mechanics* (Oxford, New York, 2001).
[15] B. A. Camley and F. L. H. Brown, Phys. Rev. E. **84**, 021904 (2011).
[16] S. Ramadurai, A. Holt, V. Krasnikov, G. van den Bogaart, J. A. Killian, and B. Poolman, J. Am. Chem. Soc. **131**, 12650 (2009).
[17] P. Cicuta, S. L. Keller, and S. L. Veatch, J. Phys. Chem. B **111**, 3328 (2007).
[18] B. D. Hughes, B. A. Pailthorpe, and L. R. White, J. Fluid Mech. **110**, 349 (1981).
[19] H. A. Stone and H. M. McConnell, Proc. R. Soc. London, Ser. A **448**, 97 (1995).
[20] B. A. Camley, C. Esposito, T. Baumgart, and F. L. H. Brown, Biophys. J. **99**, L44 (2010).
[21] M. Haataja, Phys. Rev. E. **80**, 020902R (2009).
[22] K. Inaura and Y. Fujitani, J. Phys. Soc. Jpn **77**, 114603 (2008).
[23] A. R. Honerkamp-Smith, B. Machta, and S. Keller, e-print arXiv:1104.2613v1.
[24] D. K. Lubensky and R. E. Goldstein, Phys. Fluids **8**, 843 (1996).
[25] V. Prasad, S. Koehler, and E. Weeks, Phys. Rev. Lett. **97**, 176001 (2006).
[26] Z. H. Nguyen, M. Atkinson, C. S. Park, J. Maclennan, M. Glaser, and N. Clark, Phys. Rev. Lett. **105**, 268304 (2010).
[27] M. Edidin, Annu. Rev. Biophys. Biomol. Struct. **32**, 257 (2003).
[28] K. Simons and W. L. Vaz, Annu. Rev. Biophys. Biomol. Struct. **33**, 259 (2004).
[29] S. L. Veatch and S. L. Keller, Biophys. J. **85**, 3074 (2003).
[30] S. L. Veatch and S. L. Keller, Biochim. Biophys. Acta. **1746**, 172 (2005).
[31] M. Yanagisawa, M. Imai, T. Masui, S. Komura, and T. Ohta, Biophys. J. **92**, 115 (2007).
[32] D. Saeki, T. Hamada, and K. Yoshikawa, J. Phys. Soc. Jpn **75**, 013602 (2006).
[33] M. H. Jensen, E. J. Morris, and A. C. Simonsen, Langmuir **23**, 8135 (2007).
[34] M. Laradji and P. S. Kumar, J. Chem. Phys. **123**, 224902 (2005).
[35] S. Ramachandran, S. Komura, and G. Gompper, Eur. Phys. Lett. **19**, 56001 (2010).
[36] B. A. Camley and F. L. H. Brown, Phys. Rev. Lett. **105**, 148102 (2010).
[37] J. Fan, T. Han, and M. Haataja, J. Chem. Phys. **133**, 235101 (2010).
[38] V. M. Kendon, M. E. Cates, I. Pagonabarraga, J.-C. Desplat, and P. Bladon, J. Fluid Mech. **440**, 147 (2001).
[39] G. Gonnella, E. Orlandini, and J. M. Yeomans, Phys. Rev. E. **59**, R4741 (1999).
[40] R. DeKoker, Ph.D. dissertation, Stanford University, 1996.
[41] K. Seki, S. Ramachandran, and S. Komura, Phys. Rev. E. **84**, 021905 (2011).
[42] S. Ramachandran, S. Komura, and G. Gompper, Europhys. Lett. **89**, 56001 (2010).
[43] N. Vladimirova, A. Malagoli, and R. Mauri, Phys. Rev. E. **60**, 6968 (1999).
[44] H. Tanaka and T. Araki, Phys. Rev. Lett. **81**, 389 (1998).
[45] D. Jacqmin, J. Comput. Phys. **155**, 96 (1999).
[46] T. Koga and K. Kawasaki, Phys. Rev. A **44**, R817 (1991).
[47] S. Keller and C. Stanich, personal communication (March 8, 2011).
[48] C. Esposito, A. Tian, S. Melamed, C. Johnson, S.-Y. Tee, and T. Baumgart, Biophys. J. **93**, 3169 (2007).
[49] R. Dimova, C. Dietrich, A. Hadjiisky, K. Danov, and B. Pouligny, Eur. Phys. J. B **12**, 589 (1999).
[50] E. P. Petrov and P. Schwille, Biophys. J. **94**, L41 (2009).
[51] N. Oppenheimer and H. Diamant, Phys. Rev. E. **82**, 041912 (2010).
[52] H. Stone and A. Ajdari, J. Fluid. Mech. **369**, 151 (1998).
[53] P. C. Hohenberg and B. I. Halperin, Rev. Mod. Phys. **49**, 435 (1977).
[54] K. Kawasaki and T. Ohta, Physica A **118**, 175 (1983).
[55] N. G. Van Kampen, *Stochastic Processes in Physics and Chemistry* (North Holland, Amsterdam, 2007).
[56] D. L. Ermak and J. A. McCammon, J. Chem. Phys. **69**, 1352 (1978).
[57] In order to convert between results with the $\delta_{\mathbf{k},-\mathbf{k}'}$ correlation and the δ_{ij} correlation, it is often convenient to define $R_{\mathbf{k}} = \sum_{\mathbf{p}} G_{\mathbf{kp}} Q_{\mathbf{p}}$ with $\langle Q_{\mathbf{p}}(t) Q_{\mathbf{p}}(t')\rangle = \delta_{\mathbf{p},\mathbf{p}'}\delta(t-t')$ and thus $\sum_{\mathbf{p}} G_{\mathbf{kp}} G_{\mathbf{k}'\mathbf{p}} = \delta_{\mathbf{k},-\mathbf{k}'}$.
[58] L. Lin and F. L. Brown, Phys. Rev. E **72**, 011910 (2005).
[59] A. J. Ladd, J. Chem. Phys. **88**, 5051 (1987).